Bidentate Phosphine Ligand Based Fe₂S₂-Containing Macromolecules: Synthesis, Characterization, and Catalytic Electrochemical Hydrogen Production

Weiming Gao,[†] Jianhui Liu,*,[†] Björn Åkermark,[‡] and Licheng Sun*,[†,§]

State Key Laboratory of Fine Chemicals, Dalian University of Technology, 116012 Dalian, People's Republic of China, Department of Organic Chemistry, Arrhenius Laboratory, Stockholm University, 10691 Stockholm, Sweden, and KTH Chemistry, Organic Chemistry, Royal Institute of Technology, 10044 Stockholm, Sweden

The reaction of [Fe₂(CO)₆(μ-SCH₂)₂NCH₂CH₂N(μ-SCH₂)₂Fe₂(CO)₆] (**1**) with 1,2-bis(diphenylphosphino)ethane in the presence of Me₃NO·2H₂O affords two structurally different metallomacromolecules: a dimer of the type [{Fe₂(CO)₅(μ-SCH₂)₂NCH₂CH₂N(μ-SCH₂)₂Fe₂(CO)₅}(Ph₂PCH₂)₂] (**2**) and a tetramer species containing eight iron centers with an overall formula of [{Fe₂(CO)₆(μ-SCH₂)₂-NCH₂CH₂N(μ-SCH₂)₂Fe₂(CO)₅}₂(Ph₂PCH₂)₂] (**3**). Their structures have been determined by X-ray crystallography, showing one macrocyclic complex (**2**) and one linear complex (**3**). Electrochemical hydrogen evolution catalyzed by these two complexes with ca. 80–90 single-run turnovers is observed, indicating good potential as catalysts for future applications.

Organometallic diiron dithiolate complexes of the type [Fe₂(μ-S₂R)(CO)₆] (R = −(CH₂)₃−, −CH₂NR′CH₂−)[1] have been reported as structural models for the active site of iron-only hydrogenase. The protonation on the bridgehead nitrogen heteroatom[2,3] of the disulfide ligand offers a thermodynamically and kinetically favorable pathway for hydrogen evolution in the natural system. Although attempts to achieve closer structural models of the diiron subsite have led to the development of bimetallic iron species, structural studies and electrochemical properties of multinuclear models of the active site of iron-only hydrogenase have appeared only sporadically. A very effective iron−sulfur complex for electrochemical hydrogen evolution has been reported recently with 25 single-run turnovers during bulk electrolysis with the model complex [{(μ-SCH₂)₂NR}Fe₂(CO)₆] (R = *p*-bromobenzyl).[4] This observation has been the starting point for the extension of our work in the design and synthesis of novel systems with improved catalytic properties. A synthetic approach based on multidimensional coordination complexes obtained by self-assembly is of considerable interest. In a previous publication, we reported the preparation of a −CH₂-CH₂−-bridged tetranuclear double-Fe₂S₂ complex [Fe₂(CO)₆-(μ-SCH₂)₂NCH₂CH₂N(μ-SCH₂)₂Fe₂(CO)₆] (**1**),[5] which displayed an Fe₂S₂-capped zigzag geometry. To extend this study, we decided to use complex **1** as a building block and the bidentate phosphine ligand 1,2-bis(diphenylphosphino)-ethane (dppe) as a bridging ligand. In this contribution, we have successfully isolated two interesting complexes based on the Fe₂S₂ unit by reaction of the Fe−S complex **1** with the dppe ligand. We describe herein our results concerning complexes [{Fe₂(CO)₅(μ-SCH₂)₂NCH₂CH₂N(μ-SCH₂)₂Fe₂-(CO)₅}(Ph₂PCH₂)₂] (**2**), [{Fe₂(CO)₆(μ-SCH₂)₂NCH₂CH₂N-(μ-SCH₂)₂Fe₂(CO)₅}₂(Ph₂PCH₂)₂] (**3**), and [{Fe₂(CO)₆(μ-SCH₂)₂NCH₂CH₂N(μ-SCH₂)₂Fe₂(CO)₅}(Ph₂PCH₂CH₂PPh₂-S)] (**4**). The potential for **2** and **3** as catalytic hydrogen production centers is investigated.

Recent studies on CO/PR₃-exchange reactions suggest that the replacement of a carbonyl ligand by phosphine can be easily realized.[6,7] Thus, the reaction of **1** with dppe in the presence of Me₃NO·2H₂O (molar ratio 1:1:1) affords two different kinds of molecules: the [Fe₂S₂]₂-type complex **2** and complex **3**, which is based on a [Fe₂S₂]₄-type arrangement. In both complexes, dppe acts as a bidentate bridging ligand. Complexes **2** and **3** were purified by chromatography

* To whom correspondence should be addressed. E-mail: liujh@dlut.edu.cn (J.L.), lichengs@kth.se (L.S.).
† Dalian University of Technology.
‡ Stockholm University.
§ Royal Institute of Technology.
(1) (a) Evans, D. J.; Picket, C. J. *Chem. Soc. Rev.* **2003**, *32*, 268−275. (b) Georgakaki, I. P.; Thomson, L. M.; Lyon, E. J.; Hall, M. B.; Darensbourg, M. Y. *Coord. Chem. Rev.* **2003**, *238−239*, 255−266. (c) Rauchfuss, T. B. *Inorg. Chem.* **2004**, *43*, 14−26. (d) Sun, L.; Åkermark, B.; Ott, S. *Coord. Chem. Rev.* **2005**, *249*, 1653−1663.
(2) Wang, F.; Wang, M.; Liu, X.; Jin, K.; Dong, W.; Li, G.; Åkermark, B.; Sun, L. *Chem. Commun.* **2005**, 3221−3223.
(3) Schwartz, L.; Eilers, G.; Eriksson, L.; Gogoll, A.; Lomoth, R.; Ott, S. *Chem. Commun.* **2006**, 520−522.
(4) Ott, S.; Kritikos, M.; Åkermark, B.; Sun, L.; Lomoth, R. *Angew. Chem., Int. Ed.* **2004**, *43*, 1006−1009.
(5) Gao, W.; Liu, J.; Ma, C.; Weng, L.; Jin, K.; Chen, C.; Åkermark, B.; Sun, L. *Inorg. Chim. Acta* **2006**, *359*, 1071−1080.
(6) Gloaguen, F.; Lawrence, J. D.; Schmidt, M.; Wilson, S. R.; Rauchfuss, T. B. *J. Am. Chem. Soc.* **2001**, *123*, 12518−12527.
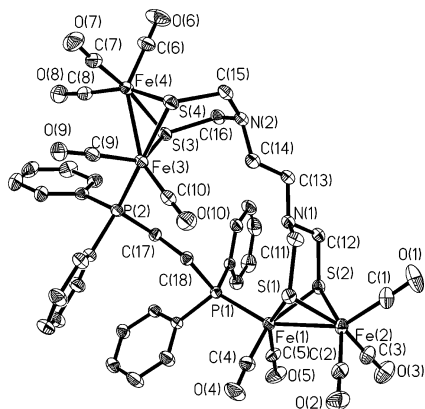(7) Gao, W.; Liu, J.; Åkermark, B.; Sun, L., manuscript submitted.

Figure 1. ORTEP view of **2** with 30% ellipsoids.

on a silica gel column, giving isolated yields of 36% and 22%, respectively. Interestingly, an unexpected side product, compound **4**, was also obtained in a yield of ca. 7%. In this species, one phosphorus atom coordinated to the iron−sulfur part and the other phosphorus atom has been converted to a noncoordinating terminal P=S group. The mechanism for the formation of the P=S bond is described elsewhere.[8]

All of the complexes have been fully characterized by mass spectrometry, IR, ^{1}H NMR, and ^{31}P NMR spectroscopies, and elemental analyses. The IR spectrum of the complex **2** displays three strong bands in the carbonyl region (2045, 1976, and 1921 cm^{-1}). Four $\nu(CO)$ bands are observed for **3** (2074, 2041, 1979, and 1927 cm^{-1}), which are related to two sets of different carbonyl stretches corresponding to carbonyls from the $[Fe_2(\mu-S_2R)(CO)_5PPh_2-]$ (2041, 1979, and 1927 cm^{-1}) and the $[Fe_2(\mu-S_2R)(CO)_6]$ (2074 cm^{-1}) moieties. The smaller IR difference (2045, 1976, and 1921 cm^{-1} vs 2041, 1979, and 1927 cm^{-1}) for the $[Fe_2(\mu-S_2R)(CO)_5PPh_2-]$ units in both **2** and **3** indicates that there is a negligible electronic distinction between the Fe_2S_2 centers in **2** and **3**. IR data for **4** also show $[Fe_2(\mu-S_2R)(CO)_5PPh_2-]$-type carbonyl stretching vibrations. A strong absorption for the P=S bond located at 693 cm^{-1} is observed as found for other similar P=S complexes.[8] Complex **1** shows a singlet, typical for a NCH_2S at 3.54 ppm, while complex **2** gives two similar singlets at 2.37 and 2.61 ppm of equal intensity. For complex **3**, NCH_2S signals are observed at 2.52, 2.64, and 3.39 ppm (1:1:2 integration). The corresponding ^{31}P NMR spectra recorded in CDCl$_3$ display one singlet relative to the dppe ligand at 60.46 ppm for **2** and 59.95 ppm for **3**, at about the same value found for other related Fe_2S_2 complexes coordinated with the dppe ligand.[8] The little change of $\Delta\delta = 0.51$ ppm also provides the fact that the interaction is weak between $[Fe_2(\mu-S_2R)(CO)_6]$ and $[Fe_2(\mu-S_2R)(CO)_5PPh_2-]$ moieties.

Single-crystal X-ray data for the complexes **2** and **3** have been obtained (Figures 1 and 2). For the macrocyclic complex **2**, the molecular structure is based upon a tetranuclear semisquare with a ring size of 14 atoms. The dppe ligand is coordinated to the iron atom via the two phosphorus atoms to form a 14-membered ring. In **2**, one phosphine atom
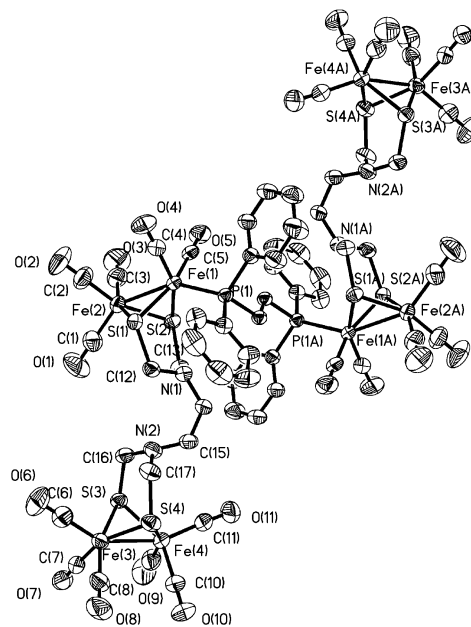
(8) Gao, W.; Ekström, J.; Liu, J.; Chen, C.; Eriksson, L.; Weng, L.; Åkermark, B.; Sun, L., manuscript submitted.

Figure 2. ORTEP view of **3** with 30% ellipsoids.

of dppe occupies an apical position and the other one is in a basal position of the Fe_2S_2 unit. The surprising basal configuration attributes to a small distortion along the chain −NCH$_2$CH$_2$N− in comparison with the single-crystal structure of **1**.[5] The Fe(1)−Fe(2) distance (2.5197 Å) is a little shorter than that of Fe(3)−Fe(4) (2.5387 Å), elongated by ca. 0.01 and 0.03 Å, respectively, compared with the Fe−Fe distance (2.5062 Å) of **1** after partial rotation. Complex **3** consists of an octanuclear structure of the type $[\{Fe_2(CO)_6-(\mu-SCH_2)_2NCH_2CH_2N(\mu-SCH_2)_2Fe_2(CO)_5\}_2(Ph_2PCH_2)_2]$, where the two $[Fe_2(CO)_6(\mu-SCH_2)_2NCH_2CH_2N(\mu-SCH_2)_2Fe_2(CO)_5]$ units are linked by a single dppe unit. The two phosphorus atoms coordinate to two iron atoms in an anti mode for the $[Fe_2S_2(CO)_5N]dppe[Fe_2S_2(CO)_5N]$ unit but in a syn manner for the $[Fe_2S_2(CO)_5(CH_2CH_2)Fe_2S_2(CO)_6]$ unit. The dppe ligand occupies the two apical positions. The midpoint of the −CH$_2$CH$_2$− bond in dppe acts as an inversion center. The Fe(1)−Fe(2) distance (2.5183 Å) is longer than that of Fe(3)−Fe(4) (2.4864 Å) and almost the same as that of Fe(1)−Fe(2) in **2**. All of the phenyls in **2** and **3** are positioned to minimize steric hindrance.

The electrochemical properties of model complexes **1**−**3** were studied by cyclic voltammetry in dry CH$_2$Cl$_2$. For **1** and **2**, irreversible reduction peaks were observed at −1.73 and −2.08 V (vs the ferrocene/ferrocenium, Fc/Fc$^+$, couple), respectively.[9] Upon the addition of excess triflic acid to CH$_2$Cl$_2$ solutions of **1** or **2** (1 mM), an additional reduction peak appeared at about −1.28 V for both compounds, 50 and 400 mV more positive than those reported for the complex $[\{(\mu-SCH_2)_2NR\}Fe_2(CO)_6]$ (R = p-bromobenzyl) under similar acidic conditions. Other reduction peaks are observed at

(9) CH$_2$Cl$_2$ was used for better solubility of **2** and **3** in it for cyclic voltammetry measurement. The different solvent systems were compared by using $[\{(\mu-SCH_2)_2NR\}Fe_2(CO)_6]$ (R = p-bromobenzyl) as a referent agent, which is reduced at −1.56 V vs Fc/Fc$^+$ in MeCN.[4] In our system and under otherwise identical conditions, this complex is reduced at −1.74 V, which gives rise to a ΔE value of 0.18 V brought by CH$_2$Cl$_2$.

around −1.70 and −2.00 V for **1** and **2**, respectively, with the current intensity increasing and shifting to more negative potential as the acid concentration are increased. These features are indicative of the presence of a catalytic proton reduction.[10,11] For complex **3**, the irreversible reduction peaks occur at −1.71 and −2.02 V, which are close to the values obtained for **1** and **2**. In the presence of excess triflic acid, the reduction peak at around −1.28 V is observed again, while the reduction peak at around −2.00 V is increased and moves to a more negative potential with an increase of the acid concentration. In addition, its current intensity is considerably higher than that of the reduction peak at around −1.70 V.[12] This provides further evidence that the PPh$_2$-coordinated Fe$_2$S$_2$ parts contribute dominantly to catalyzing the electrochemical proton reduction to molecular hydrogen. Additional information was obtained from NMR experiments. When ca. 30 equiv of HOTf are added to complex **3**, the ^{1}H NMR peak at 3.39 ppm associated with the N*CH*$_2$S grouping coordinated to the hexacarbonyl fragment is still observed; however, the peaks of the N*CH*$_2$S moieties that are coordinated to PPh$_2$-coordinated Fe$_2$S$_2$ originally observed at 2.52 and 2.64 ppm have completely shifted to ca. 4.26−4.67 ppm. The chemical−electrochemical−chemical−electrochemical (CECE) mechanism is strongly proposed. Because of the increased electron density brought by the phosphine ligand, it is first protonated on the bridging *nitrogen* atom and then on iron atoms of the PPh$_2$-coordinated Fe$_2$S$_2$ units during the CC (chemical and chemical) steps in the CECE mechanism. Further proof can also be obtained from controlled potential electrolysis.

Controlled potential electrolysis in CH$_2$Cl$_2$−Bu$_4$NPF$_6$ was performed to test the catalytic activities for complexes **1**−**3**. The complex [{(μ-SCH$_2$)$_2$NR}Fe$_2$(CO)$_6$] (R = *p*-bromobenzyl) was used as a reference for its hitherto best electrochemical hydrogen evolution activity with 25 turnovers (Figure S5).[4,13] In the absence of FeS catalysts, the initial electrolysis rate at −2.10 V is only a little higher than that at −1.70 V, both of which show a slow proton reduction

(Figure S5). For complex [{(μ-SCH$_2$)$_2$NR}Fe$_2$(CO)$_6$] (R = *p*-bromobenzyl), the rate of electrolysis slows down with time as the proton concentration decreases, and after approximately 60 min, the total charge passed through the cell approaches its maximum of 50 F, which is the equivalent of 25 turnovers. It achieves its maximum quantum in ca. 1 h. For complexes **1**−**3**, the initial electrolysis rates are almost identical in the first 20 min, the rates of electrolysis are essentially unchanged for complexes **2** and **3**, and they are only slightly lower for complex **1** during our electrolysis in 60 min. The rates of **2** and **3** are almost the same, indicating that the two terminal hexacarbonyl Fe$_2$S$_2$ units do not contribute significantly to the catalytic process. After continuous electrolysis for ca. 30 min further for complexes **1**−**3**, the rate of electrolysis slows down rapidly and becomes in agreement with the initial baseline at ca. −1.70 or −2.10 V. The data indicate that after about 1.5 h complex **1** produces ca. 60 turnovers of dihydrogen and complexes **2** and **3** can both give out ca. 80−90 turnovers. Taking the dimer structure of complexes **1** and **2** into consideration, each Fe$_2$S$_2$ unit will give ca. 30 and 40−45 turnovers, respectively. Though their efficiencies are still rather low compared with the nature hydrogenase enzymes with rates up to 6000 turnovers per second quoted (30 °C),[14] the fact that the present catalysts are not derived from expensive platinum metals stimulates us to continue our investigations in this direction.

In conclusion, we have obtained two iron−sulfur complexes. The complexes exhibited totally different topological structures, with **2** having a quasi-square structure and **3** being a three-dimensional macromolecule. The compounds show promising catalytic properties for the formation of hydrogen, and we are currently trying to connect them to photosensitizers to realize light-induced hydrogen production.

Supporting Information Available: Experimental details and crystallographic information files (CIF) for **2** and **3**. This material is available free of charge via the Internet at http://pubs.acs.org.

IC061258E

(10) Bhugun, I.; Lexa, D.; Savéant, J.-M. *J. Am. Chem. Soc.* **1996**, *118*, 3982−3983.

(11) Gloaguen, F.; Lawrence, J. D.; Rauchfuss, T. B.; Bénard, M.; Rohmer, M.-M. *Inorg. Chem.* **2002**, *41*, 6573−6582.

(12) Differential pulse voltammograms were performed to investigate the change of the reduction peaks when an excess HOTf was added (see the Supporting Information).

(13) Gloaguen, F.; Lawrence, J. D.; Rauchfuss, T. B. *J. Am. Chem. Soc.* **2001**, *123*, 9476−9477.

(14) Adams, M. W. W. *Biochim. Biophys. Acta* **1990**, *1020*, 115−145.